Conformational equilibrium and orientational ordering: ¹H-nuclear magnetic resonance of butane in a nematic liquid crystal

James M. Polson

Department of Physics, University of British Columbia, 6224 Agricultural Road, Vancouver, V6T 1Z1 Canada

E. Elliott Burnell

Department of Chemistry, University of British Columbia, 2036 Main Mall, Vancouver, V6T 1Z1 Canada

(Received 1 May 1995; accepted 17 July 1995)

In this study we use multiple-quantum 1 H-NMR spectroscopy to study butane, the simplest flexible alkane, dissolved in a nematic solvent. An analysis of the highly accurate 1 H dipolar coupling constants gives important information about conformational and orientational behavior, including the trans-gauche energy difference, E_{tg} , and the conformer probabilities and order parameters. An essential component of the analysis involves the use of mean-field models to describe the orientational ordering of solutes in a nematic solvent. Several models were found to adequately describe the molecular ordering, including the chord model of Photinos $et\ al.\ [D.\ J.\ Photinos,\ E.\ T.\ Samulski,\ and\ H.\ Toriumi,\ J.\ Phys.\ Chem.\ 94,\ 4688\ (1990)]$ and recent versions of a model proposed by Burnell and co-workers $[D.\ S.\ Zimmerman\ and\ E.\ E.\ Burnell,\ Mol.\ Phys.\ 78,\ 687\ (1993)]$. It was found that E_{tg} lies in the range $2.1-3.0\ kJ/mol$, which is significantly below most experimental estimates of the gas-phase value. An attempt to describe more realistically the conformational states by including torsional fluctuations about the rotational isomeric states did not significantly improve the quality of the fits or alter the results. Finally, the anisotropic component of the solute-solvent interaction was found to perturb only marginally the conformational probabilities from the isotropic values. $©\ 1995\ American\ Institute\ of\ Physics$.

I. INTRODUCTION

Butane is the simplest flexible alkane, possessing only one conformational degree of freedom, and has been the subject of many studies, both experimental and theoretical/ computational, concerned with the influence of condensed phases on the equilibrium conformational behavior of nonrigid molecules. Early on, Flory had suggested that the average potential of hydrocarbon molecules should closely correspond to the unperturbed form with the configurational space populated according to the Boltzmann distribution over intramolecular energy with intermolecular effects being ignored. Later, this view was challenged by Chandler et al. whose rigorous statistical mechanical theory of hydrocarbon systems predicted an increase in the gauche conformer population as a result of short-range packing in the liquid.^{2,3} There is an extensive experimental evidence to support the latter view. Gas phase studies typically report the trans-gauche energy, E_{tg} , to be 3.3–3.7 kJ/mol, ^{4–8} though a recent FTIR study has suggested that it may be as low as 2.9 kJ/mol.⁹ Experimental studies of butane, both as liquid and dissolved in other isotropic liquid solvents, consistently report lower values of E_{tg} , generally in the range 2.1–2.5 kJ/mol. $^{10-12}$

The effect of a condensed phase environment on the conformational equilibrium of butane has also been studied extensively using molecular dynamics (MD) and Monte Carlo (MC) computer simulations. These studies have generated less consistent and often confusing results over the last two decades. The earliest MD simulations of liquid butane ^{13,14} and of butane in liquid carbon tetrachloride ¹⁵ appeared to indicate that there was a significant shift toward higher *gauche* populations. Another MD study of liquid butane

found a negligible effect,¹⁶ as did the MC simulations of Jorgensen^{17–19} who cited insufficient run time and inadequate convergence as explanations for the apparent MD shortcomings. Improved MD calculations were later conducted and again suggested a significant solvent effect on conformer populations.^{20–22} In this case it was argued that the MC calculations were in error since they had employed a strong attractive methyl–methyl potential which may neutralize the packing effects.²² More recent MD and MC calculations have again concluded that there is no significant shift.^{23,24} Another recent study suggests that the conformational behavior of butane is highly sensitive to minor details in the molecular structure and the intermolecular forces used in the calculations.²⁵

An understanding of the behavior of flexible hydrocarbons in condensed phases is particularly important in the field of liquid crystals. Most molecules that form liquid crystal phases have hydrocarbon chains that are attached to rigid cores. These alkyl tails appear to be an important component of the orienting mechanism for the mesogens. Knowledge about the conformational and orientational behavior of alkanes in nematic liquid crystals then should contribute to an understanding of the ordering of liquid crystals. The behavior of longer alkanes in anisotropic fluids has been the subject of several recent NMR studies. While early NMR studies had relied on an analysis of quadrupolar coupling constants of deuterated alkanes, 26-28 recent advances in twodimensional NMR techniques combined with random deuteration of the chains have made it possible to measure the dipolar couplings between proton pairs, greatly increasing amount of information available

systems. $^{29-33}$ A detailed analysis of the dipolar couplings for alkanes ranging from hexane to decane were used to study the effects of the nematic environment on their conformational equilibria. $^{32-34}$ These studies indicate that there is a shift toward higher populations of conformers with more *gauche* bonds, an effect corresponding to a lowering in E_{tg} relative to the gas phase values, similar to that observed for butane in isotropic liquids. Moreover, this effect appeared to result from the isotropic "solvent pressure" of the condensed phase: The anisotropic component of the solute–solvent interaction was found to influence only marginally the conformer probabilities by favoring elongated conformers slightly. Similar results were found in a MD study of hexane incorporated as a solute in a model liquid–crystal solvent. Solvent.

An essential component in the analyses in the NMR studies discussed above involves the use of mean-field models to describe the orientation of molecules in a nematic environment. These models are used to calculate the molecular order parameters for each conformer, which are, in turn, used to calculate the experimental dipolar coupling constants. Thus, the ability of each model to fit the experimental couplings may be used to provide a critical test of each model. One orientational model, developed by Burnell and coworkers, describes the interaction between solute and liquid crystal as arising from the size and shape anisotropy of the solute.^{36–41} The study by Rosen *et al.*³³ concluded that early versions of this model^{37,38} were inferior to the chord model, developed by Photinos et al., 42,34,43 in which C-C bond orientations relative to the director, and correlations between orientations of neighboring C-C bonds, were the key factors in the molecular ordering. Another approximation used in the anlayses of these studies was the three-state rotational isomeric state (RIS) model¹ to describe the accessible conformational states of each C-C torsion bond of the molecule. Although its application permits a convenient analysis of the data, it was judged to be a severe approximation. Later, it was shown that the inclusion of torsion-angle fluctuations about the RIS trans and gauche states can significantly improve the quality of the fits.⁴⁴

In this paper, we present a multiple-quantum (MQ) ¹H-NMR study of butane in a nematic liquid crystal. We view this study as an extension of previous experimental and computational work on the effect of condensed phases on the conformational behavior of butane, and as a continuation of the study of alkyl chain behavior in a specifically anisotropic fluid. The simplicity of this alkane offers some advantages. First, the NMR spectrum of butane is sufficiently simple that, with the help of straightforward MQ experiments, its analysis is possible without the need to resort to either specific or random deuteration. In this way, one may measure the dipolar coupling constants much more precisely than was done for the longer alkanes. As well, assumptions necessary for longer alkanes, such as the equivalence of the internal rotational potential for all C-C bonds along the chain, are unnecessary. One goal of this study is the determination of E_{to} for butane in a condensed phase, and its dependence on both isotropic and anisotropic contributions from the solutesolvent interactions. However, since the use of mean-field models to describe the molecular orientation in a nematic liquid crystal is a key part of the analysis, an equally important aspect of this work is the investigation of the model dependence of the results. The influence of both the mean-field model and the details of the geometry, including the *trans-gauche* dihedral angle and the RIS approximation, are discussed.

II. THEORETICAL BACKGROUND

A. Dipolar coupling constants

NMR has proven to be an excellent technique to study the conformational behavior and orientational ordering of molecules in anisotropic fluids. Most studies to date that have investigated the behavior of hydrocarbons have used $^2\text{H-NMR}$ spectroscopy to measure quadrupolar splittings, $\Delta\,\nu_Q$, of C– ^2H bonds of deuterated molecules. The $^2\text{H-NMR}$ spectra consist of a set of doublets, each with a splitting given by

$$\Delta \nu_Q = \frac{3e^2qQ}{4h} S_{C-D}, \qquad (1)$$

where the order parameter S_{C-D} is given by

$$S_{C-D} = \langle \frac{3}{2} \cos^2 \theta_{C-D} - \frac{1}{2} \rangle \tag{2}$$

and where θ_{C-D} is the angle that the $C^{-2}H$ bond makes with the static magnetic field, along which the nematic phase director is aligned. Thus, the 2H -NMR spectra readily provide information through S_{C-D} about orientational ordering of individual methylene segments along alkyl chains. On the other hand, the $\Delta\nu_Q$'s provide no direct information about intermethylene correlations. Also, the number of distinct $\Delta\nu_Q$'s is limited to the number of independent carbon units along the chain. Thus, the information contained in quadrupolar couplings tends to be inadequate for studies in which detailed information about molecular orientational ordering and conformational behavior is sought.

Dipolar coupling constants, by contrast, provide much more detailed information about flexible molecules. The dipolar coupling constant between protons i and j on a partially oriented molecule is given by

$$D_{ij} = -\frac{\gamma^2 \hbar \mu_0}{8 \pi^2} \left\langle \frac{\frac{3}{2} \cos^2 \theta_{ij}^Z - \frac{1}{2}}{r_{ij}^3} \right\rangle, \tag{3}$$

where r_{ij} is the internuclear distance and θ_{ij}^Z is the angle between the internculear vector and the static magnetic field. The factor of r_{ij}^{-3} is significant because it provides information about the average distance between methylene groups on flexible alkyl chains. This feature, as well as information about the average orientation of internuclear vectors resulting from the dependence on θ_{ij}^Z , causes the D_{ij} to be highly sensitive to the molecular conformation and orientation. As well, there are many more independent dipolar coupling constants than quadrupolar coupling constants, greatly increasing the information about molecular properties that may be extracted from the experimental data. In the case of butane, there are seven independent D_{ij} 's and only two $\Delta \nu_Q$'s.

Although there is a clear advantage in determining dipolar coupling constants, these are often difficult to obtain in all but the simplest molecules. The complexity of the ¹H onequantum NMR spectrum of partially oriented molecules increases rapidly with the size and complexity of the corresponding moleculr spin system. In large molecules, including the nematogens themselves which have $\gtrsim 20^{-1}$ H spins, the large number of spectral lines results in severe overlap in which individual lines cannot be resolved, rendering any spectral analysis impossible. In molecules of intermediate complexity such as butane, this is not a major problem; however, the spectrum is still sufficiently complex as to hinder its analysis. In such cases, it is useful to analyze first high-order multiple-quantum (MQ) spectra. Such spectra have far fewer associated transitions, a feature that makes it much easier to assign lines of trial simulated spectra to those of the experimental spectra. The dipolar coupling constants obtained as fitted parameters may then be used as a starting point in the analysis of the one-quantum spectrum. The dipolar coupling constants obtained in the second stage of analysis are highly accurate. We have shown the usefulness of multiple-quantum spectroscopy as a tool in the analysis of one-quantum spectra for molecules of intermediate complexity in previous studies on the structural determination of the eight-spin molecule biphenylene⁴⁵ and the six-spin molecule 1,3-dichloro-2ethenylbenzene.46

A significant alternative to this method that is suitable and necessary for molecules of greater complexity is the approach taken by Pines and co-workers. ^{29–33} In this case, random deuteration of the molecules, combined with MQ-filtered COSY NMR experiments and ²H double-quantum decoupling, were used to obtain spectra that are essentially superpositions of subspectra comprised to a single splitting. These subspectra arise from isotopic species that have a single pair of protons and therefore yield directly the D_{ij} associated with each proton pair. This technique was used successfully to measure dipolar coupling constants for a series of oriented alkanes in a study^{32,33} that is highly relevant to the present work and on which we shall comment further.

B. Flexibility

A common approach to analyzing dipolar coupling constants of partially oriented flexible molecules is to assume that the molecule exists in several discrete conformations, each of which has its own distinct Saupe order matrix. This assumption is justified as long as the correlation time associated with the reorientation of the molecule, τ_R , and the rate of exchange, k, between the different conformations satisfy $k\tau_R \ll 1$. An important model used for approximating the conformations of hydrocarbon chains is Flory's rotational isomeric state (RIS) model in which each C-C torsion bond is assumed to exist in three states, *trans* and $\pm gauche$, with dihedral angles of 0° and $\pm \phi_g$, respectively, corresponding to the angles at the minima of the rotational potential profile. These two approximations form the basis for the analysis of the D_{ij} 's in the present study, as described below.

One can show that an experimentally measured dipolar coupling constant between protons i and j for a flexible molecule satisfying the condition described above is given by

$$D_{ij} = \frac{2}{3} \sum_{n} p^{n} \sum_{\alpha\beta} S_{\alpha\beta}^{n} D_{ij,\alpha\beta}^{n}, \qquad (4)$$

where p^n is the probability of the *n*th conformer, and where $S^n_{\alpha\beta}$, the Saupe order matrix for the *n*th conformer, is defined by

$$S_{\alpha\beta}^{n} = \langle \frac{3}{2} \cos \theta_{\alpha,Z}^{n} \cos \theta_{\beta,Z}^{n} - \frac{1}{2} \delta_{\alpha\beta} \rangle, \tag{5}$$

where $\theta_{\alpha,Z}^n$ is the angle between the α -molecular axis of the nth conformer and the nematic director, which, for many liquid crystals, is aligned with the static magnetic field along the Z axis. $D_{ij,\alpha\beta}^n$ is a tensor defined by

$$D_{ij,\alpha\beta}^{n} = -\frac{\mu_0 \gamma^2 \hbar}{8 \pi^2 r_{ii}^3} \left(\frac{3}{2} \cos \theta_{\alpha}^{ij,n} \cos \theta_{\beta}^{ij,n} - \frac{1}{2} \delta_{\alpha\beta} \right), \quad (6)$$

where $\theta_{\alpha}^{ij,n}$ is the angle between the internuclear vector \mathbf{r}_{ij} and the *n*th α -molecular axis.

C. The mean-field potential and E_{ta}

A useful approach to the analysis of the dipolar coupling constants is to model the solute energy with a mean-field potential, $U_n(\omega)$, which is a function of both the conformation and the orientation of the solute in the uniaxial nematic solvent. The potential can be divided into

$$U_n(\omega) = U_{\text{int},n} + U_{\text{ext},n}(\omega), \tag{7}$$

where $U_{\rm int,n}$ is the internal energy associated with the conformational state of an isolated molecule, and $U_{\rm ext,n}(\omega)$ is the orientationally dependent energy of interaction between the solute and the external mean field. The latter term can written in terms of a spherical harmonics expansion which can be used to define the isotropic, $U_{\rm ext,n}^{\rm iso}$, and anisotropic, $U_{\rm ext,n}^{\rm aniso}(\omega)$, components of the external field:

$$U_n^{\text{ext}}(\boldsymbol{\omega}) = c_{0,0}^n Y_{0,0} + \sum_{l=2}^{\text{even}} \sum_{m=-l}^{l} c_{l,m}^n Y_{l,m}(\boldsymbol{\theta}, \boldsymbol{\phi})$$

$$\equiv U_{\text{ext},n}^{\text{iso}} + U_{\text{ext},n}^{\text{aniso}}(\boldsymbol{\omega}). \tag{8}$$

Note that the odd terms in the expansion for $U_{\text{ext},n}^{\text{aniso}}(\omega)$ vanish as a result of the apolarity of the nematic phase. Also, since $U_{\text{int},n}$ is purely isotropic, we shall omit the "ext" subscript on the anisotropic component of the external potential energy, $U_n^{\text{aniso}}(\omega)$, since only the external component of the solute energy has an associated anisotropy. The isotropic component of the full solute potential energy, therefore, is the sum of internal and external contributions:

$$U_n^{\text{iso}} = U_{\text{int},n}^{\text{iso}} + U_{\text{ext},n}^{\text{iso}}.$$
 (9)

We define the effective trans-gauche energy difference, E_{tg} , as the difference in the total isotropic potential energy for the trans and gauche states of the butane molecule:

$$E_{tg} = U_{gauche}^{\text{iso}} - U_{trans}^{\text{iso}}$$

$$= E_{tg}^{\text{int}} + E_{tg}^{\text{ext}}, \qquad (10)$$

where E_{tg}^{int} is the internal energy difference between the *trans* and *gauche* states, and where

$$E_{tg}^{\text{ext}} = U_{\text{ext},gauche}^{\text{iso}} - U_{\text{ext},trans}^{\text{iso}}$$
 (11)

is the external perturbation to the internal energy difference due to the condensed phase environment.

The anisotropic component of the mean field, $U_n^{\rm aniso}(\omega)$, gives rise to the orientational ordering of the solute in the nematic environment. The elements of the Saupe order tensor for each conformer may be calculated by

$$S_{\alpha\beta}^n$$

$$= \frac{\int (\frac{3}{2}\cos\theta_{\alpha,Z}^{n}\cos\theta_{\beta,Z}^{n} - \frac{1}{2}\delta_{\alpha\beta})\exp(-U_{n}^{\text{aniso}}(\omega)/kT)d\omega}{\int \exp(-U_{n}^{\text{aniso}}(\omega)/kT)d\omega}.$$
(12)

One can show that the conformer probabilities can be written as

$$p^{n} = \frac{G^{n} \exp(-U_{n}^{\text{iso}}/kT) \int \exp(-U_{n}^{\text{aniso}}(\omega)/kT) d\omega}{\sum_{n} G^{n} \exp(-U_{n}^{\text{iso}}/kT) \int \exp(-U_{n}^{\text{aniso}}(\omega)/kT) d\omega},$$
(13)

where $G^n = \sqrt{I_{xx}^n I_{yy}^n I_{zz}^n}$ is a rotational kinetic energy factor, dependent on the principal values of the moment of inertia tensor for each conformer, $I_{\alpha\alpha}^n$, that arises from marginalizing out the molecular angular momenta from the full singlet probability distribution for flexible molecules. Equation (13) clearly shows the dependence of the conformer probabilities on the anisotropic mean-field potential.

D. Modeling of $U_n^{aniso}(\omega)$

In order to extract conformational and orientational information from the experimental dipolar coupling constants using the relations described above, it is necessary to employ a suitable model for the anisotropic potential, $U_n^{\mathrm{aniso}}(\omega)$. This is required since, in the limit of fast internal exchange between conformers, the conformer probabilities and molecular order parameters appear as products in the expression for D_{ii} in Eq. (4), and cannot be determined separately in a fit. Using a model for $U_n^{\text{aniso}}(\omega)$, however, the dipolar coupling constants may be calculated by optimizing the model parameters and E_{tg} , which generally are separately determinable, in the fit of the experimental D_{ij} . The p^n and $S_{\alpha\beta}^n$ are calculated using Eqs. (12) and (13). In the present study, we restrict the analysis to models that are characterized by a single parameter. We feel that this is a necessary restriction since we are limited to only seven independent ¹H dipolar coupling constants for butane. As well, by employing a wide variety of orientational models, we hope to bound E_{tg} to a limited range of values and thereby obtain a modelindependent estimate of this quantity.

Below, we review briefly the important features of the models used in this study. More detailed descriptions may be found in the references cited.

1. Model A: Size and shape potentials

Burnell and co-workers have developed a series of related mean-field models for the orientational potential of solutes of arbitrary nature in a nematic liquid crystal.^{36–41} All of these models treat the solute as a collection of van der Waals spheres placed at the atomic sites in the molecule in order to

approximate the molecular structure. It is the anisotropy in the shape of the solute interacting with the unaxial nematic field that gives rise to the orientation dependence of the potential energy. There are six different varieties of this "size and shape" (SS) interaction that we describe below. First, however, there are two important considerations that we discuss

- (1) The general mean-field model developed by Burnell and co-workers consists of a contribution from the longrange interaction between the molecular electric-quadrupole moment (EQM) with the average electric field gradient (EFG) of the liquid crystal, in addition to the short-range SS interactions that we consider here. There is direct evidence of the EQM-EFG interaction in the case of 2H_2 , where it is the dominant orienting mechanism. $^{49-51}$ In addition, it was shown that one can construct liquid crystal mixtures in which the average EFG sampled by ²H₂ vanishes.⁵² These zero-EFG mixtures were the nematic liquid crystals chosen for the experiments in which the SS potentials were developed, since the model predicts that in this case the EQM-EFG interaction vanishes, leaving the short-range interaction as the sole mechanism responsible for solute orientation. While it is true that the average EFG experienced by an arbitrary solute will not be the same as that experienced by ²H₂ or any other solute, the high quality of the fits to experimental order parameters calculated under this assumption suggests that it is a reasonable approximation, though there has been some recent criticism of this claim. 53 Therefore, we use a zero-EFG nematic mixture in the present study, in keeping with these considerations. Previous studies of alkane behavior in liquid crystals that employed two of these models did not use a zero-EFG mixture nor comment at all on this matter.^{32,33}
- (2) It is very important to note that in all of the SS potentials developed by Burnell and co-workers, there is a residual isotropic component; that is,

$$\langle U_{SS}^{n} \rangle = c_{0,0}^{n} Y_{0,0} = \frac{1}{4\pi} \int U_{SS}^{n}(\omega) d\omega \neq 0,$$
 (14)

where $U_{\rm SS}(\omega)$ represents any of the mean-field potentials discussed by Burnell and co-workers based on solute size and shape anistropy that we discuss below. The residual isotropic component presents no difficulties in the case of rigid solutes where it has no effect at all on the predicted order parameters since these quantities depend strictly on the purely anisotropic component of the potential, $U_n^{\rm aniso}(\omega)$. The situation for flexible molecules is quite different. Inspection of Eq. (13) clearly shows that in calculating the conformer probabilities, any isotropic component contained in a mean-field potential used to model the supposedly anisotropic $U_n^{\rm aniso}(\omega)$ will be absorbed into the calculated $U_n^{\rm iso}$, and will thus affect the resulting value of E_{tg} . Thus, an improperly calculated $E_{tg}^{\rm false}$ will be obtained, where

$$E_{tg}^{\text{false}} = E_{tg} + \langle U_{\text{SS}}^{trans} \rangle - \langle U_{\text{SS}}^{gauche} \rangle. \tag{15}$$

This point was not considered in any of the previous studies of oriented flexible molecules that used a SS model, and calls into question the values for E_{tg} that were obtained. We return to this point later in the discussion section of this paper. To

calculate properly the conformer probabilities, it is necessary simply to subtract out the isotropic component of $U_{\rm SS}$:

$$U_n^{\text{aniso}}(\omega) = U_{\text{SS}}^n(\omega) - \langle U_{\text{SS}}^n \rangle. \tag{16}$$

Model A_I . This is the original SS model, in which the mean-field orientation-dependent potential energy is given by³⁷

$$U_{SS}^{n}(\omega) = \frac{1}{2}k(C_{n}(\omega))^{2}, \tag{17}$$

where $C_n(\omega)$ is the minimum circumference traced out by the projection of the solute onto a plane perpendicular to the nematic director

Model A_2 . This model is a slight variation of A_1 :³⁷

$$U_{SS}^{n}(\omega) = \frac{1}{2}k(D_{n}(\omega))^{2}, \tag{18}$$

where $D_n(\omega)$ is the maximum circumference traced out by the projection of the solute onto the plane perpendicular to the nematic director.

Model A_3 . This two-parameter model was the first extension of A_1 in which³⁸

$$U_{SS}^{n}(\omega) = \frac{1}{2}k(C_{n}(\omega))^{2} - \frac{1}{2}\xi kC_{n}(\omega)Z_{n}(\omega),$$
 (19)

where $Z_n(\omega)$ is the length of the projection of the solute along the nematic director. In order to use this as a one-parameter model, we fix the second parameter to ξ =3.9, the value obtained from a fit to the order parameters for a collection of 46 solutes using this model in which both k and ξ were treated as free parameters.³⁶ This should be a valid assignment since the model parameters associated with a particular zero-EFG mixture are, in principle, solute independent.

Model A_4 . The model potential is given by 36

$$U_{\rm SS}^{n}(\omega) = -\frac{1}{2} k_s \int_{Z_{\rm min}, n}^{Z_{\rm max}, n} C_n(Z, \omega) dZ, \qquad (20)$$

where Z is the position along the nematic director bounded by the minimum, $Z_{\min,n}$, and maximum, $Z_{\max,n}$, points of the orientation-dependent projection of the solute along this axis. $C_n(Z,\omega)$ is the minimum circumference traced out by the solute at position Z along the director. Thus, $C_n(Z,\omega)dZ$ is the area of an infinitesmally thin ribbon that traces out this circumference, and the integral is the area of the full projection of the surface of the molecule onto a plane parallel to the nematic director. Thus A_4 can be interpreted as an anisotropic surface potential. Note that the equation for A_4 is a generalization of the second term for the potential A_3 which can be obtained if one neglects the Z dependence of $C_n(Z,\omega)$ and sets all values equal to $C_n(\omega)$. This model is similar to another by Ferrarini et al.⁵⁴ in which surface area elements of the van der Waals spheres contribute an energy proportional to $P_2(\cos \psi)ds$, where ψ is the angle between a surface element normal and the nematic director, and ds the area of the surface element. In model A_4 , the interaction energy effectively is proportional to $\sin \psi ds$.

Model A_5 . This model is a combination of models A_1 and A_4 :

$$U_{SS}^{n}(\omega) = \frac{1}{2} k(C_{n}(\omega))^{2} - \frac{1}{2} k_{s} \int_{Z_{\min,n}}^{Z_{\max,n}} C_{n}(Z,\omega) dZ.$$
 (21)

Again, it is necessary to fix the ratio of parameters to the value obtained from the previous study by Zimmerman et al., 36 where $k_s/k = 23.529$. Note that this particular model was the most successful for predicting order parameters for molecules oriented in a zero-EFG liquid crystal mixture.

Model A_6 . The potential is given by 36

$$U_{SS}^{n}(\omega) = 2k_{xy}A_{xy}^{n}(\omega) - k_{z}D_{n}(\omega)Z_{n}(\omega), \qquad (22)$$

where, again, $D_n(\omega)$ is the maximum circumference traced out by the projection of the solute onto the plane perpendicular to the nematic director Z axis, and Z_n is the length of the projection of the solute along the Z axis. Also, A_{xy}^n is the area of the projection contained within the maximum circumference, $D_n(\omega)$. For this study, we fix $k_z/k_{xy}=0.327$, the optimal value obtained in Ref. 36. Note that the quality of the fit to experimental order parameters for the solutes in that study using A_6 was comparable to the best fit obtained using A_5 .

2. Model B: Moment of inertia model

Model B uses a mean-field potential based on the expansion of $U_n^{\rm aniso}(\omega)$ in Eq. (8) truncated to second rank:

$$U_n^{\text{aniso}}(\omega) = \sum_{m=-2}^{2} c_{2,m}^n Y_{2,m}(\theta, \phi).$$
 (23)

The expansion coefficients, $c_{2,m}^n$, are parametrized by using a model developed by Straley⁵⁵ in which the interacting molecules are represented by parallelepipeds. The symmetry of the parallelepipeds causes this expansion to be reduced to^{32,33}

$$U_n^{\text{aniso}}(\omega) = c_{2,0}^n Y_{2,0} + \sqrt{\frac{3}{2}} c_{2,2}^n \sin^2(\theta) \cos(2\phi). \tag{24}$$

For a solute modeled as a parallelepiped of length, L, width, W, and breadth, B:

$$c_{2,0}^{n} = \frac{1}{3} \epsilon \left[6LBW + L(W^{2} + B^{2}) - 2W(L^{2} + B^{2}) - 2B(W^{2} + L^{2}) \right], \tag{25}$$

$$c_{2,2}^{n} = \frac{\epsilon}{\sqrt{6}} [(L^{2} - BW)(B - W)],$$
 (26)

for $L \ge W \ge B$, where ϵ is a parameter that characterizes the solute-solvent interaction. The parallelepiped dimensions can be calculated in terms of the principal-axis components of the moment of inertia tensor, $I_{\alpha\beta}^n$, for each conformer, n:²⁸

$$D_{\alpha} = 2\sqrt{\frac{5(I_{\beta\beta}^{n} + I_{\gamma\gamma}^{n} - I_{\alpha\alpha}^{n})}{2m}},$$
(27)

where L, B, and W are written as the elements D_{α} .

3. Model C: The chord model

Photinos, Samulski, and co-workers have developed a mean-field model for molecular orientation in a uniaxial phase that is specially tailored for molecules comprised of repeating identical units. Thus, it is not surprising that this model gives remarkably good results in the analysis of H dipolar coupling constants of oriented hydrocarbons. 33,34,44 Indeed Rosen *et al.* 33 concluded this to be the

superior model in their study of oriented alkanes. This potential is derived from the leading terms in a rigorous expansion of the mean-field interaction. Photinos *et al.*³⁴ write

$$U_n^{\text{aniso}}(\boldsymbol{\omega}) = -\sum_{i=1} \left[\tilde{w}_0 P_2(\mathbf{s}^i, \mathbf{s}^i) + \tilde{w}_1 P_2(\mathbf{s}^i, \mathbf{s}^{i+1}) \right], \quad (28)$$

where \mathbf{s}^i is a unit vector describing the orientation of the *i*th C-C bond of the hydrocarbon chain, and where the sum is over all of the bonds in the chain. The factors $P_2(\mathbf{s}^i, \mathbf{s}^{i+m})$ are given by

$$P_2(\mathbf{s}^i, \mathbf{s}^{i+m}) = \frac{3}{2}\cos\theta_Z^i \cos\theta_Z^{i+m} - \frac{1}{2}\mathbf{s}^i \cdot \mathbf{s}^{i+m}, \tag{29}$$

where θ_Z^i is the angle between the *i*th bond and the nematic director, which aligns with the static magnetic field direction along the Z axis. The parameters, \tilde{w}_m , are proportional to the liquid crystal order parameter. The first term in Eq. (28) corresponds to the independent alignment of separate C-C bonds that may arise, for example, from the anisotropy of the polarizability of the bonds.⁵⁶ The second term incorporates correlations between adjacent-bond orientations, and therefore distinguishes between conformations that may have equal numbers of trans and gauche bonds but significantly different shapes; thus, it accounts for shape-dependent excluded-volume interactions. In the present study, we consider the specific case, $\tilde{w}_0 = \tilde{w}_1$. This is called the "chord model," since it can be shown to be equivalent to a model in which the chords connecting the midpoints of the C–C bonds are the elemental submolecular units interacting with the external field.

The mean-field potential defined in Eq. (28) can be written in a more convenient form. Following Rosen *et al.*,³³ we define the components of a second rank tensor:

$$u_{\alpha\beta} = -2\tilde{w}_0 \sum_{i} \left[T_{\alpha\beta}(\mathbf{s}^i, \mathbf{s}^i) + \frac{1}{2} (T_{\alpha\beta}(\mathbf{s}^i, \mathbf{s}^{i+1}) + T_{\alpha\beta}(\mathbf{s}^{i+1}, \mathbf{s}^i)) \right], \tag{30}$$

where

$$T_{\alpha\beta}(\mathbf{s}^{i},\mathbf{s}^{i+m}) = s_{\alpha}^{i} s_{\beta}^{i+m} - \frac{1}{3} \delta_{\alpha\beta} \mathbf{s}^{i} \cdot \mathbf{s}^{i+m}, \tag{31}$$

where s_{α}^{i} is the α component of the *i*th C-C bond vector. The principle-axis components of $u_{\alpha\beta}$, $u_{33} \ge u_{22} \ge u_{11}$, can be used to parameterize the leading terms in the expansion

$$U_n^{\text{aniso}}(\omega) = c_{2,0}^n Y_{2,0} + \sqrt{\frac{3}{2}} c_{2,2}^n \sin^2(\theta) \cos(2\phi)$$
 (32)

according to

$$u_{2,0}^{n} = \frac{1}{\sqrt{6}} \left(2u_{33} - (u_{11} + u_{22}) \right), \tag{33}$$

$$u_{2,2}^{n} = \frac{1}{2}(u_{22} - u_{11}). \tag{34}$$

E. Other details of the calculations

1. Torsional fluctuations

While the RIS model provides a convenient method for the analysis of experimental data to obtain information about the conformational behavior of hydrocarbons, the high quality of the experimental dipolar coupling constants that may be obtained for the systems means that the crudeness of this approximation may be the limiting factor of the accuracy with which information can be determined. The principle restriction of this model is the limitation of the dihedral angle, ϕ , to the three angles, 0° , $\pm \phi_{g}$, associated with the trans and ±gauche states. Thus, it would be useful to examine the role of torsional fluctuations of ϕ about these minima of the rotational potential energy. A simple approach is offered in a study by Photinos et al.44 in which the dihedral angle can assume values at $\pm \Delta \phi$ about the RIS state values, in addition to the RIS values themselves. For butane, this corresponds to nine conformers with dihedral panels of $\phi = 0^{\circ}$, $\pm \Delta \phi$, $\pm \phi_g$, and $\pm (\phi_g \pm \Delta \phi)$. We use this extended-RIS model in addition to the regular RIS model to determine the importance of torsional fluctuations on the determined E_{to} , conformer probabilities and molecular order parameters. We fix the population ratios of each extended-RIS triplet to 1:2:1 and set $\Delta \phi = 20^{\circ}$ to approximate roughly the shape of each peak in the torsional probability distribution.

2. The dihedral angle, ϕ_g

Experimental estimates of the dihedral angle, ϕ_g , vary widely, ranging from 110° from an electron diffraction study⁵⁷ to a value of 118° obtained from an analysis of the Raman spectrum.⁶ Because the dipolar couplings have a sensitive dependence on ϕ_g , we examine the variation in the results of our analysis to changes in ϕ_g .

3. Methyl groups

Since four of seven butane dipolar coupling constants involve protons in methyl groups, it is important to model the rotation of these groups in a reasonable way. We employ a methyl group rotation barrier of 12.5 kJ/mol and sample different molecular geometries in steps of 5°, with probabilities weighted by the Boltzmann factor.

III. EXPERIMENT

A liquid-crystal mixture of 55 wt % Merck ZLI 1132 and 45 wt % N-(p-ethoxybenzylidene)-p'-n-butylaniline (EBBA) was prepared. Approximately 500 mg of the mixture was placed into a 5 mm o.d. standard NMR tube and was thoroughly degased through several freeze-pump-thaw cycles. Enough gaseous butane was condensed into the tube at a liquid nitrogen temperature to achieve a \approx 5 mol % solute liquid-crystal ratio under the assumption that all of the gas dissolved in the liquid crystal. The tube was then flame-sealed under vacuum. Since a fraction of the gas in the tube filled the space above the sample, the true solute concentration was <5 mol %. To provide a lock, the NMR tube was equipped with a capillary tube, filled with acetone- d_6 , that was held coaxial to the NMR tube with teflon spacers.

The ¹H-NMR spectra were acquired on a Bruker AMX-500 spectrometer at 301.4 K at 500 MHz. The MQ spectra were acquired using the following pulse sequence:

$$\left(\frac{\pi}{2}\right) - \tau - \left(\frac{\pi}{2}\right) - t_1 - \left(\frac{\pi}{2}\right) - \tau' - t_2 \text{(acquire)}.$$

To detect selectively a $\pm n$ -quantum spectrum, the phase ϕ of the first two pulses relative to the third pulse were cycled through 2n steps in increments of π/n with alternating addition and subtraction of the signal for each value of t_1 . Thus, the acquisition of the seven-quantum spectrum required a phase cycle employing 14 steps of 25.7°, while that of the eight-quantum used 16 steps of 22.5° increments.

Both spectra were acquired using a preparation time, τ , of 12 ms, a recycle delay of 3.5 s, and a t_1 increment time of 41.7 μ m, which corresponds to an f_1 sweep width of 24 kHz. There were 1250 increments of t_1 collected for the seven-quantum spectrum and 1200 increments for the eight-quantum spectrum. For both spectra, a delay of $\tau'=1$ ms was used to minimize the contribution of the liquid-crystal signal that is generated after the third pulse. For every t_1 increment, there were 1024 data points collected in t_2 . The total time for acquisition of each spectrum was approximately 20 h.

Both data sets were zero-filled to 2048 in the t_1 dimension prior to the 2D magnitude Fourier-transform. Each MQ spectrum was obtained by performing a summed projection of the 2D spectrum onto the f_1 axis. Peak positions of both the one-quantum and MQ spectra were calculated using the Bruker UXNMR peak-peaking routine. The one-quantum spectrum was analyzed using the computer program LEQUOR;⁵⁹ the MQ spectra were analyzed using a suitably modified version of LEQUOR.

IV. RESULTS AND DISCUSSION

A. NMR spectra

The experimental one-quantum spectrum of partially oriented butane is shown in the lower half of Fig. 1(a). The ¹H-NMR spectrum of butane consists of a thick mass of lines spanning a frequency range of 10 kHz with essentially no notable features and sits on the broad liquid-crystal ¹H spectrum. A horizontally expanded region of the spectrum is shown in the lower half of Fig. 1(b). It is apparent that while the spectral-line density is high, overlap is not so severe as to make it impossible to determine the frequencies of most of the lines; thus, a fit of the experimental spectrum is certainly possible. However, the complexity of the spectrum makes it extremely difficult to do so without very accurate initial estimates of the coupling constants and chemical shifts. Small deviations from the true values of these parameters would alter the line frequencies and intensities enough to generate a spectrum with significantly different fine structure from that of the experimental spectrum.

These problems can be circumvented with the help of MQ spectra. The seven-quantum and eight-quantum spectra for oriented butane are shown in Fig. 2. There are fewer lines than appear in the one-quantum spectrum spread out over a comparable frequency range. The strategy used to fit these spectra employed the model A_5 described earlier, with parameters optimized to the zero-EFG liquid–crystal mixture according the results of an earlier study³⁶ to predict molecular order parameters and thus dipolar coupling constants. A value for E_{tg} of 3.0 kJ/mol was used to generate initial conformer probabilities. Chemical shifts and J-coupling constants were initialized to their isotropic values.⁶⁰ The trial

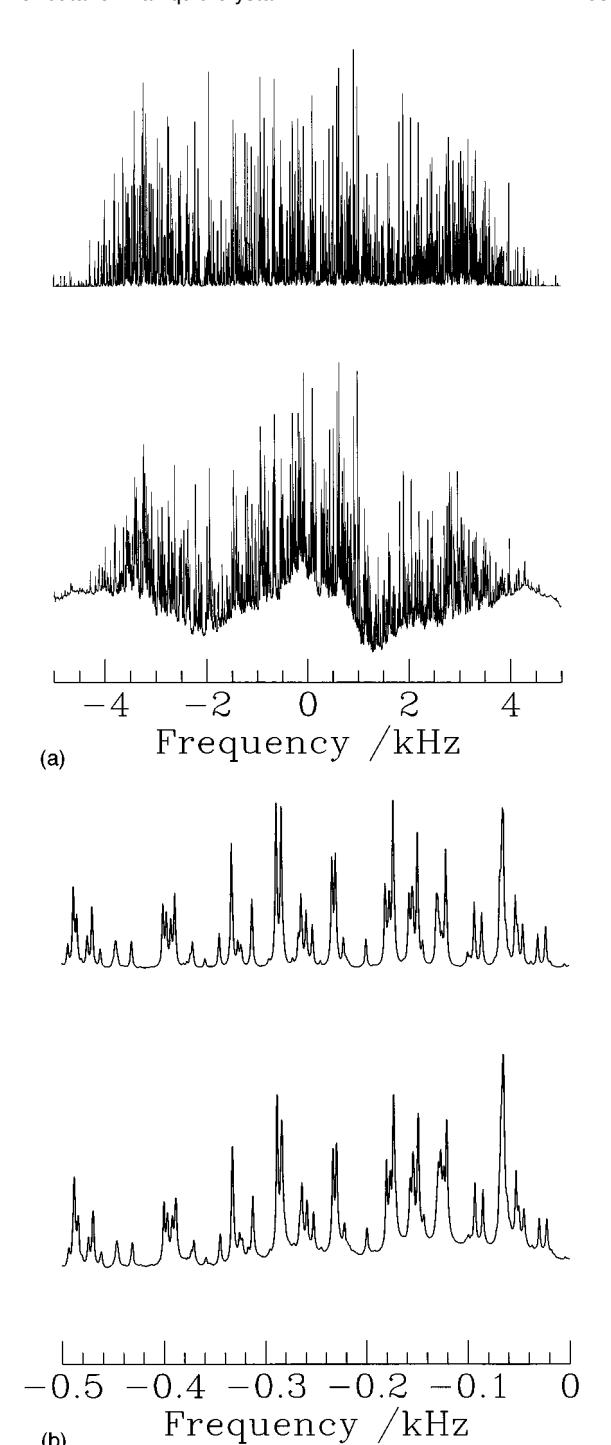
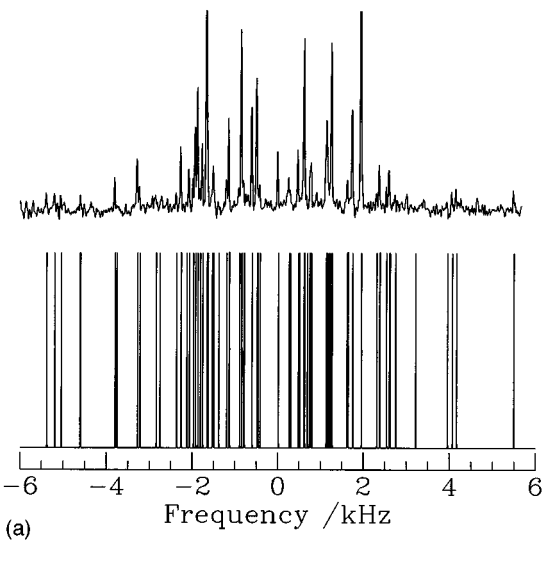


FIG. 1. (a) Experimental (bottom) and simulated (top) spectra of partially oriented butane. (b) Expanded region of the spectra in (a).

spectrum that was generated provided an adequate starting point to fit simultaneously the two MQ spectra. In total, 19 lines from the eight-quantum spectrum and 35 lines from the seven-quantum spectrum were fit successfully. Figure 2 shows the frequencies of all of the lines calculated in the fit of the MQ spectra. A large number of these lines in the experimental seven-quantum spectrum have very weak intensity and are barely discernable, if at all, from the fluctuations in the noise. Note that the line intensities have a very complex and sensitive dependence on the preparation time,



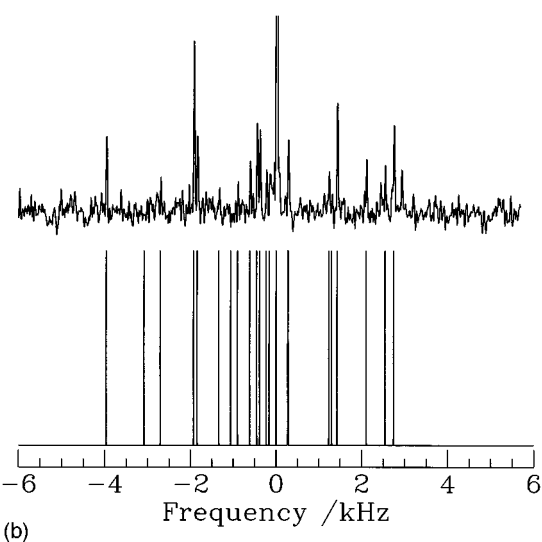


FIG. 2. (a) Experimental (top) and simulated (bottom) seven-quantum spectra of partially oriented butane. (b) Experimental (top) and simulated (bottom) eight-quantum spectra of partially oriented butane. For the simulated spectra of (a) and (b), the line intensities have been arbitrarily set equal since the intensity of each MQ transition is a complicated function of the preparation time τ and the parameters in the spin Hamiltonian, and does not provide any information for the present study.

 τ . Ideally one uses an optimum τ , if one exists, for which all of the associated MQ coherences are appreciably populated. A practical approach is to coadd a series of spectra acquired with different values of τ . In the present case, we found the spectra acquired with a single τ to be sufficient.

The trial one-quantum spectrum that was predicted from the fit of the MQ spectra proved to be an excellent starting point in the fit of the experimental one-quantum spectrum; assignment of spectral lines was tedious, but trivial. A simulated one-quantum spectrum using the fitted dipolar coupling constants, chemical shift difference and *J* couplings is shown in Fig. 1(a) with the experimental spectrum. The high quality of the fit is more evident in the expanded plot of a region of the spectrum shown in Fig. 1(b). Table I lists the final values of the fitting parameters obtained in both the one-quantum and MQ spectral fits. The protons are labeled according to

TABLE I. Fitting parameters (Hz) from the multiple-quantum and one-quantum spectral fits.

Parameter	MQ	1Q
D_{12}	817.8 ±0.2	817.63±0.03
D_{14}	-199.6 ± 0.2	-199.57 ± 0.05
D_{16}	-389.2 ± 0.2	-388.84 ± 0.02
D_{18}	-196.4 ± 0.2	-196.14 ± 0.02
D_{45}	1601.3 ± 0.3	1601.09 ± 0.04
D_{46}	65.3 ± 0.5	65.61 ± 0.08
D_{47}	34.5 ± 0.5	33.98 ± 0.08
$\delta_1 - \delta_4$	309.5 ± 0.2	309.40 ± 0.07
${J}_{14}$	7.4 ^a	7.37±0.05
J_{16}	-0.2^{a}	-0.19 ± 0.02
J_{46}	5.7 ^a	6.04 ± 0.02
J_{47}	8.6ª	8.83±0.02

^aIsotropic values from Ref. 60.

Fig. 3. Note that the predicted coupling constants and chemical shift difference are almost exactly the same for both fits; the *J* couplings are shifted only slightly from their literature values. Thus, an analysis of the MQ spectra for this particular ten-spin system is shown to provide information sufficiently accurate for the type of analysis that we describe below. This is a significant point when questioning the accuracy of MQ-spectral information of molecules of slightly greater complexity for which the one-quantum spectrum cannot be analyzed.

B. Conformational and orientational behavior of butane

Table II summarizes the results of the fit of the experiment dipolar coupling constants using the eight mean-field models described in Sec. II, for three different ϕ_g dihedral angles, with and without corrections for torsional fluctuations about the RIS states. Among the SS models, A_1 , A_2 , and A₃ yield fits of comparable quality, with root-meansquare (rms) deviations of approximately 30 Hz, regardless of the variation in the geometrical parameters. Models A_4 , A_5 , and A_6 yield fits of substantially improved quality with rms values roughly half those of the fits with the other three models. This trend is entirely consistent with the results of the study of Zimmerman et al.³⁶ in which these SS models were tested on a series of rigid solutes oriented in the same zero-EFG liquid-crystal mixture. This probably is due to the fact that models A_4 , A_5 , and A_6 incorporate much more detail into their descriptions of the molecular size and shape than do the others. Model B yielded by far the poorest fit of the experimental dipolar coupling constants. This is surpris-

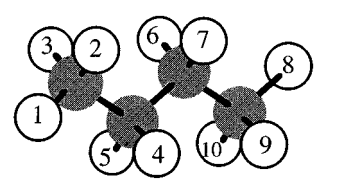


FIG. 3. Diagram of the *trans* conformer of butane showing the labeling of the protons.

TABLE II. Results of the fits to the experimental dipolar coupling constants.

		$\phi_g = 112^{\circ}$		$\phi_g = 116^{\circ}$		$\phi_g = 120^{\circ}$	
Model		$\Delta \phi = 0^{\circ}$	20°	$\Delta \phi = 0^{\circ}$	20°	$\Delta \phi = 0^{\circ}$	20°
$\overline{A_1}$	$E_{tg}/\text{kJ mol}^{-1}$	2.22	2.22	2.33	2.34	2.43	2.45
	$k/10^3 \text{ N m}^{-1}$	5.81	5.92	5.75	5.86	5.69	5.80
	rms/Hz	32	32	29	29	26	26
A_2	$E_{tg}/\text{kJ mol}^{-1}$	2.35	2.36	2.43	2.45	2.50	2.54
=	$k/10^3 \text{ N m}^{-1}$	4.64	4.74	4.62	4.72	4.60	4.69
	rms/Hz	34	33	30	30	27	27
A_3	$E_{tg}/\text{kJ mol}^{-1}$	2.27	2.26	2.37	2.38	2.47	2.49
5	$k/10^3 \text{ N m}^{-1}$	4.74	4.81	4.70	4.77	4.66	4.73
	rms/Hz	32	32	29	29	26	27
A_4	$E_{tg}/\text{kJ mol}^{-1}$	2.58	2.67	2.74	2.84	2.90	3.01
•	$k_s/10^3 \text{ N m}^{-1}$	70.4	71.0	68.8	69.6	67.2	68.1
	rms/Hz	17	15	19	19	22	20
A_5	$E_{tg}/\text{kJ mol}^{-1}$	2.48	2.54	2.62	2.68	2.75	2.82
	$k_s/10^3 \text{ N m}^{-1}$	46.4	47.0	45.6	46.2	44.7	45.4
	rms/Hz	17	15	16	14	17	15
A_6	$E_{tg}/\text{kJ mol}^{-1}$	2.62	2.70	2.78	2.85	2.93	3.01
	$k_{xy}/10^3 \text{ N m}^{-1}$	18.5	18.7	18.1	18.3	17.7	18.0
	rms/Hz	13	12	15	14	18	17
В	$E_{tg}/\text{kJ mol}^{-1}$	2.94	3.07	3.18	3.32	3.46	3.59
	$\epsilon/10^4 \text{ kJ m}^{-3}$	4.50	4.56	4.37	4.44	4.23	4.32
	rms/Hz	44	41	48	44	52	48
C	$E_{tg}/\mathrm{kJ}\;\mathrm{mol}^{-1}$	2.09	2.09	2.15	2.17	2.22	2.26
	$\tilde{w_0}$ /kJ mol ⁻¹	0.736	0.744	0.725	0.734	0.713	0.723
	rms/Hz	12	11	9	7	9	7

ing in light of the results of Rosen $et~al.^{33}$ in which this model yielded particularly good fits, especially so for the shorter alkanes. Model C gave the best fit, consistent with the results of Rosen et~al. and as one may expect for a model specially tailored for molecules composed of identical repeating units. The quality of the fits for all mean-field models is generally insensitive to the value of ϕ_g , and is only marginally improved by incorporating torsional fluctuations into the fits. Table III lists the experimental and calculated dipolar coupling constants for all of the mean-field models for the case of $\phi_g = 116^\circ$ and $\Delta \phi = 20^\circ$ and clearly highlights the relative success of each model in describing the orientational ordering of butane. Note that the simulated dipolar coupling constants for all models do not fall within the uncertainties of the highly accurate experimental coupling constants. This

discrepancy is due to a variety of factors, including small uncertainties in the molecular geometry, molecular vibrations, as well as the limitations in the mean-field models themselves.

The principal goal of the present study is an accurate determination of E_{tg} , the effective energy difference between the *trans* and *gauche* states of butane in an anisotropic condensed phase. The results summarized in Table II clearly show that the value for this quantity obtained from an analysis of dipolar coupling constants is sensitive to the model used to describe the orientational ordering. Model C yields an E_{tg} of ≈ 2.1 kJ/mol, the lowest estimate of any of the models. Model B gives the highest value, with $E_{tg} \approx 2.9 - 3.6$ kJ/mol, while the various SS models predict values that lie between these two extremes. Thus, the esti-

TABLE III. Experimental and calculated dipolar coupling constants (Hz) for $\phi_g = 116^{\circ}$ and $\Delta \phi = 20^{\circ}$.

$\overline{D_{ij}}$	Experimental	A_1	A_2	A_3	A_4	A_5	A_6	В	С
$\overline{D_{12}}$	817.3	842.9	822.5	843.0	821.7	829.8	822.5	776.6	821.8
D_{14}	-199.6	-195.3	-207.9	-194.7	-211.3	-206.2	-207.9	-206.5	-192.2
D_{16}	-388.8	-392.2	-360.5	-393.5	-352.6	-366.6	-360.5	-339.4	-390.0
D_{18}	-196.1	-229.2	-199.9	-229.2	-198.7	-208.7	-199.9	-160.6	-203.0
D_{45}	1601.1	1536.2	1609.1	1535.1	1615.3	1588.7	1609.1	1700.9	1591.0
D_{46}	65.6	70.1	63.5	70.8	66.1	67.9	63.5	66.0	66.5
D_{47}	34.0	66.8	42.0	67.1	34.3	46.4	42.0	-13.4	52.7
rms		29	30	29	19	14	14	44	7

TABLE IV. Nematic (N) and isotropic (I) phase trans probabilities.

		$\phi_g = 112^{\circ}$		$\phi_g = 116^{\circ}$		$\phi_g = 120^{\circ}$	
Model	Phase	$\Delta \phi = 0^{\circ}$	20°	$\Delta \phi = 0^{\circ}$	20°	$\Delta \phi = 0^{\circ}$	20°
A_1	N	0.547	0.549	0.559	0.561	0.570	0.573
	I	0.537	0.539	0.549	0.551	0.560	0.544
A_2	N	0.559	0.562	0.562	0.572	0.577	0.582
2	I	0.550	0.552	0.559	0.562	0.567	0.572
A_3	N	0.551	0.553	0.563	0.565	0.573	0.576
,	I	0.541	0.543	0.553	0.555	0.563	0.567
A_4	N	0.580	0.590	0.596	0.607	0.612	0.624
4	I	0.573	0.584	0.589	0.600	0.606	0.618
A_5	N	0.571	0.606	0.585	0.592	0.599	0.607
3	I	0.563	0.570	0.577	0.585	0.591	0.599
A_6	N	0.585	0.592	0.600	0.608	0.615	0.624
0	I	0.577	0.586	0.592	0.602	0.609	0.618
В	N	0.615	0.629	0.638	0.652	0.664	0.677
2	I	0.608	0.622	0.632	0.646	0.658	0.671
C	N	0.535	0.537	0.543	0.546	0.551	0.555
Ü	I	0.523	0.526	0.531	0.534	0.538	0.544

mates for E_{tg} are spread over a fairly wide range. Note that while increasing the value of ϕ_g consistently leads to higher estimates of E_{tg} , the range of values obtained from each model is small compared to differences between the predictions of different models, with the exception of some of the SS models which predict very similar E_{tg} 's. Including torsional fluctuations in the calculations causes only a very slight shift toward a higher E_{tg} .

To assess the accuracy of each model prediction we must consider the quality of each fit to the experimental dipolar coupling constants. Since model B yielded such a poor fit, the high calculated E_{tg} values must be treated skeptically. The poorness of this fit relative to those for other models is emphasized in Table III. The dipolar coupling constant D_{47} , for example, which is highly sensitive to E_{tg} , is actually predicted to have a different sign from the experimental value. In light of this consideration, we exclude the range of values of E_{tg} predicted by model B. The low value of E_{tg} obtained using model C mirrors the results of Rosen et al., in which a consistently low E_{tg} for alkanes of various lengths was determined. Thus, we take 2.1 kJ/mol as the lower limit in our estimate of E_{tg} . The values for E_{tg} predicted by the SS potentials span a fairly wide range, 2.2-3.0 kJ/mol. Of particular importance are models A_5 and A_6 , which account for the oriented molecule's shape in the most detailed manner and thus yielded the best fits among the SS models. These models also gave the higher estimates of E_{tg} , with a range of 2.5–3.0 kJ/mol, and thus provide an upper limit to the estimate of E_{tg} for butane in this study. To summarize, our analysis of the ¹H dipolar coupling constants of partially oriented butane using a variety of mean-field models suggests that $E_{tg} \approx 2.1 - 3.0$ kJ/mol.

While a model-independent estimate of E_{tg} would have been preferred, the results of our analysis are significant,

nevertheless. The range 2.1–3.0 kJ/mol is below most experimental gas-phase values which lie in the range 3.3–3.7 kJ/mol,^{4–8} with the exception of the value of 2.9 kJ/mol reported in Ref. 9. Thus, our study provides evidence that *gauche*-conformer populations of butane in an anisotropic condensed phase are enhanced relative to the gas-phase values, in accord with much experimental evidence for butane in isotropic condensed phases.^{10–12}

Table IV lists the trans-state probabilities calculated for the various models employed in our analysis. As expected the probabilities increase with increasing calculated E_{to} , with model B predicting the highest probabilities and model C predicting the lowest. Considering only the successful models that were used to establish a range of values of E_{to} , we estimate that the *trans* probabilities lie in the range 0.54– 0.62. Also shown in Table IV are the trans probabilities for an isotropic phase obtained by setting $U_n^{\text{aniso}}(\omega) = 0$ in Eq. (13). The isotropic probabilities are consistently slightly lower than the nematic-phase probabilities, indicating that the anisotropy in the mean field has the effect of favoring the elongated trans state relative to the gauche states. Since these shifts are very small, it appears that the conformational distribution is essentially determined by the isotropic "solvent pressure" of the liquid crystal, in agreement with the findings of Rosen et al. for longer alkanes.

Table V summarizes the model dependence of the calculated principal axis system (PAS) order parameters for both the *trans* and *gauche* states of butane for the special case of $\phi_g = 116^{\circ}$ and $\Delta \phi = 20^{\circ}$. It is interesting to note that the calculated principal order matrix component, S_{zz} , for the *trans* state varies inversely with the calculated E_{tg} and *trans*-state probabilities. Thus, the calculated S_{zz} is lowest for model B and highest for model C. Also shown for both con-

TABLE V. Calculated principal axis system (PAS) order parameters, S_{zz} and $S_{yy}-S_{xx}$, and PAS Euler angle, $\beta_{\rm rot}$, for *trans* and *gauche* conformers of butane for ϕ_g =116° and $\Delta\phi$ =20°. For both conformers, the PAS y axis bisects the C–C–C–C dihedral angle, and the PAS z axis makes an angle of $\beta_{\rm rot}$ with the central C–C bond toward the methyl groups.

Model	Conformer	S_{zz}	$S_{yy} - S_{xx}$	$oldsymbol{eta_{ m rot}}$
$\overline{A_1}$	trans	0.177	0.007	43.6°
•	gauche	0.107	-0.037	25.6°
A_2	trans	0.175	0.010	43.3°
-	gauche	0.108	-0.035	27.2°
A_3	trans	0.177	0.006	43.5°
5	gauche	0.108	-0.037	25.7°
A_4	trans	0.151	0.034	44.6°
·	gauche	0.101	-0.616	25.0°
A_5	trans	0.160	0.025	44.1°
	gauche	0.103	-0.053	23.2°
A_6	trans	0.154	0.028	44.1°
ū	gauche	0.100	-0.059	24.3°
B	trans	0.140	0.061	42.0°
	gauche	0.078	-0.064	23.8°
C	trans	0.179	0.013	41.6°
	gauche	0.089	-0.07	23.6°

formers is the Euler angle $\beta_{\rm rot}$, defined as the angle between the central C–C bond and the principal axis system (PAS) z axis. As the results clearly show, the PAS orientation is not particularly sensitive the choice of models used to describe the orienting potential. Thus, an interesting result of these calculations is that the orientation of the PAS system predicted for each model is essentially identical to that for the PAS system of the moment of inertia tensor for both conformers, which is the axis system calculated using model B.

An important result of the present study is the fact that, with the exception of model B, all of the mean-field models for molecular orientation in a nematic phase employed here yielded physically reasonable results in the fits of the experimental dipolar coupling constants. This in marked contrast to the results of Rosen et al.33 who concluded that the SS models that were tested (models A_1 and A_3) were deficient and unable to adequately describe the orientation of flexible alkanes. One major complaint against model A_1 , for example, was that the calculated E_{tg} was unusually high, and found to increase with increasing alkane chain length. However, it is important to note that these calculations failed to account for the fact that each SS potential is not purely anisotropic, but has a residual isotropic component [see Eq. (14)] that must be subtracted away from the potentials defined in Eqs. (17)-(22) in order to calculate correctly E_{tg} . In the case of butane, failure to incorporate this correction leads to an incorrect value, E_{tg}^{false} , defined by Eq. (15), that was found to be $\approx 10\%$ higher for model A_1 compared to the correct value, a result of the fact that $\langle U_{\rm SS}^{trans} \rangle > \langle U_{\rm SS}^{gauche} \rangle$ It is entirely conceivable that this effect may become more pronounced as the shape anisotropy increases with increasing hydrocarbon chain length and yield results similar to those of Rosen et al. Their results for model A₃ contain unrealistically low values for E_{tg} . For butane it was found that $\langle U_{SS}^{trans} \rangle < \langle U_{SS}^{gauche} \rangle$, the opposite of what was observed for model A_1 as a result of the large negative term in Eq. (19), which yielded E_{tg}^{false} $< E_{tg}$. Thus, the apparent deficiencies in the SS models may arise from the failure to account for the isotropic component inherent to all of these potentials. In addition, the results of the present study strongly suggest that the more recent forms of the SS potentials are much more successful than are the earlier versions in fitting experimental dipolar coupling constants and therefore of describing the orientation of flexible molecules.

V. CONCLUSIONS

In this study, we have investigated the conformational and orientational behavior of butane aligned in a nematic liquid crystal. Information obtained from the analysis of the seven-quantum and eight-quantum ¹H-NMR spectra provided a sufficiently good starting point to analyze the highly complex one-quantum spectrum and thus to obtain extremely accurate estimates of the seven independent ¹H dipolar coupling constants. An analysis of the coupling constants was carried out with the aid of several different mean-field models for molecular orientation in a nematic environment. It was found that recent versions of the "size and shape" potential proposed by Burnell and co-workers, and, in particular, the chord model proposed by Photinos et al. were able to describe successfully the intermolecular interaction of butane in a liquid crystal, while a model based on the molecular moment of inertia tensor was found to be inadequate. An effective trans-gauche energy difference in the range of 2.1–3.0 kJ/mol was determined, suggesting that the gauchestate probabilities are enhanced in a condensed anisotropic environment relative to the gas-phase values. Varying the dihedral angle, ϕ_{g} , between trans and gauche states, and inclusion of torsional fluctuations about the internal rotational potential minima were found to have only small effects on the results. The anisotropic potential was found to cause a very minor shift toward higher probabilities of the elongated trans conformer relative to the isotropic values, in agreement studies of longer alkanes, suggesting that the conformational behavior of butane is similar to that found in the neat liquid phase.

ACKNOWLEDGMENTS

Financial support of the Natural Sciences and Engineering Research Council of Canada and the award of NSERC and Killam Graduate Scholarships to J.M.P. are gratefully acknowledged.

¹P. J. Flory, Statistical Mechanics of Chain Molecules (Wiley-Interscience, New York, 1969).

²L. R. Pratt and D. Chandler, J. Chem. Phys. **68**, 4202 (1978).

³L. R. Pratt and D. Chandler, J. Chem. Phys. **68**, 4213 (1978).

⁴ A. L. Verma, W. F. Murphy, and H. J. Bernstein, J. Chem. Phys. **60**, 1540 (1974).

⁵J. R. Durig and D. A. C. Compton, J. Phys. Chem. **83**, 265 (1979).

⁶D. A. C. Compton, S. Montero, and W. F. Murphy, J. Phys. Chem. 84, 3587 (1980).

⁷R. K. Heenan and L. S. Bartell, J. Chem. Phys. **78**, 1270 (1983).

⁸K. B. Wiberg and M. A. Murcko, J. Am. Chem. Soc. **110**, 8029 (1988).

⁹G. Gassler and W. Huttner, Z. Naturforsch. **45a**, 113 (1990).

¹⁰L. Colombo and G. Zerbi, J. Chem. Phys. **73**, 2013 (1980).

¹¹S. Kint, J. R. Scherer, and R. G. Snyder, J. Chem. Phys. **73**, 1599 (1980).

¹²D. A. Cates and A. MacPhail, J. Phys. Chem. **95**, 2209 (1991).

¹³ J. P. Ryckaert and A. Bellemans, Chem. Phys. Lett. **30**, 123 (1975).

- ¹⁴J. P. Ryckaert and A. Bellemans, Discuss. Faraday Soc. **66**, 95 (1978).
- ¹⁵ D. W. Rebertus, B. J. Berne, and D. Chandler, J. Chem. Phys. **70**, 3395 (1979).
- ¹⁶T. A. Weber, J. Chem. Phys. **69**, 2347 (1978).
- ¹⁷W. L. Jorgensen, J. Am. Chem. Soc. **103**, 677 (1981).
- ¹⁸ W. L. Jorgensen, J. Chem. Phys. **77**, 5757 (1982).
- ¹⁹ W. L. Jorgensen, J. Phys. Chem. **87**, 5304 (1983).
- ²⁰ R. Edberg, D. J. Evans, and G. P. Morriss, J. Chem. Phys. **84**, 6933 (1986).
- ²¹ P. A. Wielopolski and E. R. Smith, J. Chem. Phys. **84**, 6940 (1986).
- ²² E. Enciso, J. Alonso, N. G. Almarza, and F. J. Bermejo, J. Chem. Phys. **90**, 413 (1989).
- ²³D. Brown and J. H. R. Clarke, J. Chem. Phys. **92**, 3062 (1990).
- ²⁴ N. G. Almarza, E. Enciso, J. Alonso, F. J. Bermejo, and M. Alvarez, Mol. Phys. **70**, 1 (1990).
- ²⁵D. J. Tobias and C. L. Brooks, J. Chem. Phys. **92**, 2582 (1990).
- ²⁶ A. Ben-Shaul, Y. Rabin, and W. M. Gelbart, J. Chem. Phys. **78**, 4303 (1983).
- ²⁷D. B. Creamer, R. K. Pathria, and Y. Rabin, J. Chem. Phys. **84**, 476 (1985).
- ²⁸ B. Janik, E. T. Samulski, and H. Toriumi, J. Phys. Chem. **91**, 1842 (1987).
- ²⁹ M. Gochin, K. V. Schenker, and A. Pines, J. Am. Chem. Soc. **108**, 6813 (1986).
- ³⁰ M. Gochin, H. Zimmerman, and A. Pines, Chem. Phys. Lett. **137**, 51 (1987).
- ³¹ M. Gochin, D. Hugi-Cleary, H. Zimmerman, and A. Pines, Mol. Phys. 60, 205 (1987).
- ³² M. Gochin, A. Pines, M. E. Rosen, S. P. Rucker, and C. Schmidt, Mol. Phys. 69, 671 (1990).
- ³³ M. E. Rosen, S. P. Rucker, C. Schmidt, and A. Pines, J. Phys. Chem. 97, 3858 (1993).
- ³⁴ D. J. Photinos, B. J. Poliks, E. T. Samulski, A. F. Terzis, and H. Toriumi, Mol. Phys. **72**, 333 (1991).
- ³⁵ J. Alejandre, J. W. Emsley, D. J. Tildesley, and P. Carlson, J. Chem. Phys. 101, 7027 (1994).
- ³⁶D. S. Zimmerman and E. E. Burnell, Mol. Phys. **78**, 687 (1993).
- ³⁷ A. J. van der Est, M. Y. Kok, and E. E. Burnell, Mol. Phys. **60**, 397 (1987).

- ³⁸D. S. Zimmerman and E. E. Burnell, Mol. Phys. **69**, 1059 (1990).
- ³⁹ D. S. Zimmerman, Y. Li, and E. E. Burnell, Mol. Cryst. Liq. Cryst. **203**, 61 (1991).
- ⁴⁰ J. B. S. Barnhoorn, C. A. de Lange, and E. E. Burnell, Liq. Crystals. 13, 319 (1993).
- ⁴¹ K. Y. Li, D. S. Zimmerman, and E. E. Burnell, Mol. Phys. **78**, 673 (1993).
- ⁴²D. J. Photinos, E. T. Samulski, and H. Toriumi, J. Phys. Chem. **94**, 4688 (1990).
- ⁴³ D. J. Photinos, E. T. Samulski, and H. Toriumi, J. Phys. Chem. **94**, 4694 (1990).
- ⁴⁴D. J. Photinos, E. T. Samulski, and H. Toriumi, J. Phys. Chem. **96**, 6979 (1992).
- ⁴⁵ J. M. Polson and E. E. Burnell, J. Magn. Reson. Series A **106**, 223 (1994).
- ⁴⁶J. C. T. Rendell and E. E. Burnell, J. Magn. Reson. Series A **112**, 1 (1995).
- ⁴⁷E. E. Burnell and C. A. de Lange, J. Magn. Reson. **39**, 461 (1980).
- ⁴⁸ E. E. Burnell, C. A. de Lange, and O. G. Mouritsen, J. Magn. Reson. **50**, 188 (1982).
- ⁴⁹ J. G. Snijders, C. A. de Lange, and E. E. Burnell, Israel J. Chem. **23**, 269 (1983).
- ⁵⁰ E. E. Burnell, C. A. de Lange, and J. G. Snijders, Phys. Rev. A 25, 2339 (1982).
- ⁵¹ A. J. van der Est, E. E. Burnell, and J. Lounila, J. Chem. Soc., Faraday Trans. 2 84, 1095 (1988).
- ⁵² P. B. Barker, A. J. van der Est, E. E. Burnell, G. N. Patey, C. A. de Lange, and J. G. Snijders, Chem. Phys. Lett. **107**, 426 (1984).
- ⁵³ A. F. Terzis and D. J. Photinos, Mol. Phys. **83**, 847 (1994).
- ⁵⁴ A. Ferrarini, G. J. Moro, P. L. Nordio, and G. R. Luckhurst, Mol. Phys. 77, 1 (1992).
- ⁵⁵ J. P. Straley, Phys. Rev. A **10**, 1881 (1974).
- ⁵⁶S. Marčelja, J. Chem. Phys. **60**, 3599 (1974).
- ⁵⁷W. F. Bradford, S. Fitzwater, and L. S. Bartell, J. Mol. Struct. **38**, 185 (1977)
- ⁵⁸ A. Wokaun and R. R. Ernst, Chem. Phys. Lett. **52**, 407 (1977).
- ⁵⁹P. Diehl, P. M. Henrichs, and W. Niederberger, Mol. Phys. **20**, 139 (1971).
- ⁶⁰D. W. Aksnes and P. Albriktsen, Acta Chem. Scand. **24**, 3764 (1970).

The Journal of Chemical Physics is copyrighted by the American Institute of Physics (AIP). Redistribution of journal material is subject to the AIP online journal license and/or AIP copyright. For more information, see http://ojps.aip.org/jcpo/jcpcr/jsp Copyright of Journal of Chemical Physics is the property of American Institute of Physics and its content may not be copied or emailed to multiple sites or posted to a listserv without the copyright holder's express written permission. However, users may print, download, or email articles for individual use.

The Journal of Chemical Physics is copyrighted by the American Institute of Physics (AIP). Redistribution of journal material is subject to the AIP online journal license and/or AIP copyright. For more information, see http://ojps.aip.org/jcpo/jcpcr/jsp